

1 *Supplement of*

2

3 **Ice core nitrogen isotopes archive dramatic changes in West Antarctic**  
4 **Ice Sheet thinning**

5

6 **Amy C. F. King et al.**

7 *Correspondence to:* Amy C. F. King (amyking@bas.ac.uk)

8

9

10

11

12

13

14

15

16

17

18

19

20

21

22

23

24

25

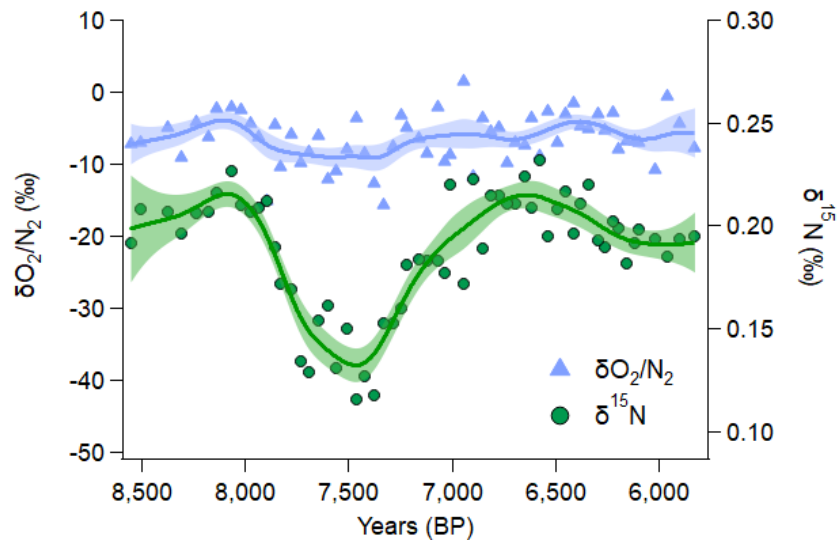
26

27

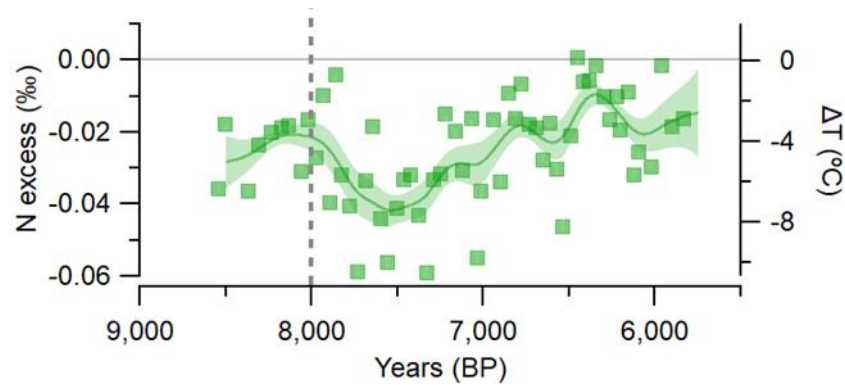
28 **Supplementary Table 1:** Summary of parameters used to generate smoothing splines and uncertainty bands for ice core  
29 records. Note that for Skytrain  $\delta^{15}\text{N}$ ,  $\delta^{40}\text{Ar}$  and  $\text{O}_2/\text{N}_2$ , spline uncertainty is given for the period 6 ka – 8.5 ka to omit  
30 unreasonable large values at the ends of the record where errors become unconstrained, and for Siple Dome data between 13.5  
31 Ka - 16 Ka. Where analytical uncertainty is unknown, i.e. for the Siple Dome data, the code is run without these values and  
32 final spline errors are therefore less conservative than if analytical uncertainty were included.

Ice Core Record	Spline Timespan (ka)	Spline data spacing (yrs)	Spline cut-off frequency (yrs)	Spline smoothing parameter	Analytical uncertainty included?	Spline average $\pm$ 1-sigma confidence interval (%)
Skytrain $\delta^{15}\text{N}$	5,000 – 9,000	1	50	1e-6	Y	0.007
Skytrain $\delta^{40}\text{Ar}$	5,000 – 9,000	1	50	1e-6	Y	0.025
Skytrain $\text{O}_2/\text{N}_2$	5,000 – 9,000	1	50	1e-6	Y	1.410
Siple Dome $\delta^{15}\text{N}$	13,000 – 17,000	1	50	2e-6	N	0.013
Siple Dome $\text{O}_2/\text{N}_2$	13,000 – 17,000	1	50	2e-6	N	1.999

33  
34  
35  
36  
37  
38  
39  
40  
41  
42  
43  
44



**Supplement Figure 1: Measured values of  $\delta\text{O}_2/\text{N}_2$  in the Skytrain record shown with  $\delta^{15}\text{N}$ . The stability of the  $\delta\text{O}_2/\text{N}_2$  record through this time period suggests that the nitrogen isotopes record is not affected by fractionation processes of gas loss.**



**Supplement Figure 2: N excess values and implied  $\Delta T$  if N excess values were interpreted as a true temperature signal in our measured ice samples.**

## 1D borehole model

We estimate the changes in temperature through time and depth by solving a 1D transient heat equation. Our model is almost identical to the one described in Jordan et al. (2018), we refer the reader to that reference for details and we simply give a summary and explain the new developments in this section.

Following Jordan et al (2018), we calculate temperature  $T$  in a dome of ice thickness  $H$  from time  $t_0$  before present and neglecting horizontal transport as:

$$\frac{\partial T}{\partial t} + w \frac{\partial T}{\partial z} - \frac{\partial T}{\partial z} \left( k \frac{\partial T}{\partial z} \right) = 0, T(z, 0) = T_0(z) \quad 0 \leq z \leq H, T(H, t) = T_s(t) \quad -t_0 \leq t \leq 0,$$

where  $k$  is the thermal diffusivity, that depends on temperature and density (Cuffey and Paterson 2010, chapter 9),  $T_s$  is the surface temperature and the vertical velocity  $w$  can be written as:

$$w(z, t) = -a(t) \frac{\rho_i}{\rho(z)} \eta(z),$$

where the relative density  $\rho$  to the density of ice  $\rho_i$  accounts for vertical compression. We assume that the vertical variability of velocity, represented by the shape function  $\eta$ , is independent of changes in time, that are proportional to surface accumulation  $a$ .

To consider the effect of changes in ice thickness through time, we introduce the normalized elevation  $e(z, t) = z/H(t)$  and, using the chain rule of derivatives, rewrite our temperature equation as:

$$\frac{\partial T}{\partial t} + (w - \dot{H}e) \frac{1}{H} \frac{\partial T}{\partial e} - \frac{1}{H^2} \frac{\partial T}{\partial e} \left( k \frac{\partial T}{\partial e} \right) = 0, T(e, 0) = T_0(e) \quad 0 \leq e \leq 1, T(1, t) = T_s(t) \quad -t_0 \leq t \leq 0,$$

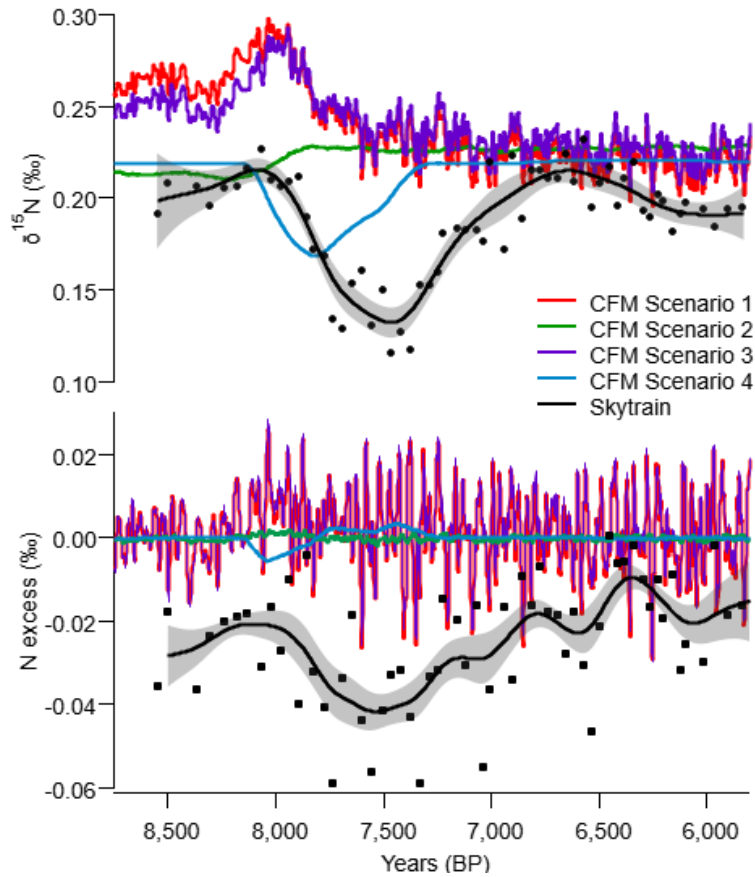
where  $\dot{H}$  is the time derivative of ice thickness. We solve the equation using a standard forward time and centred space (FTCS) finite difference method.

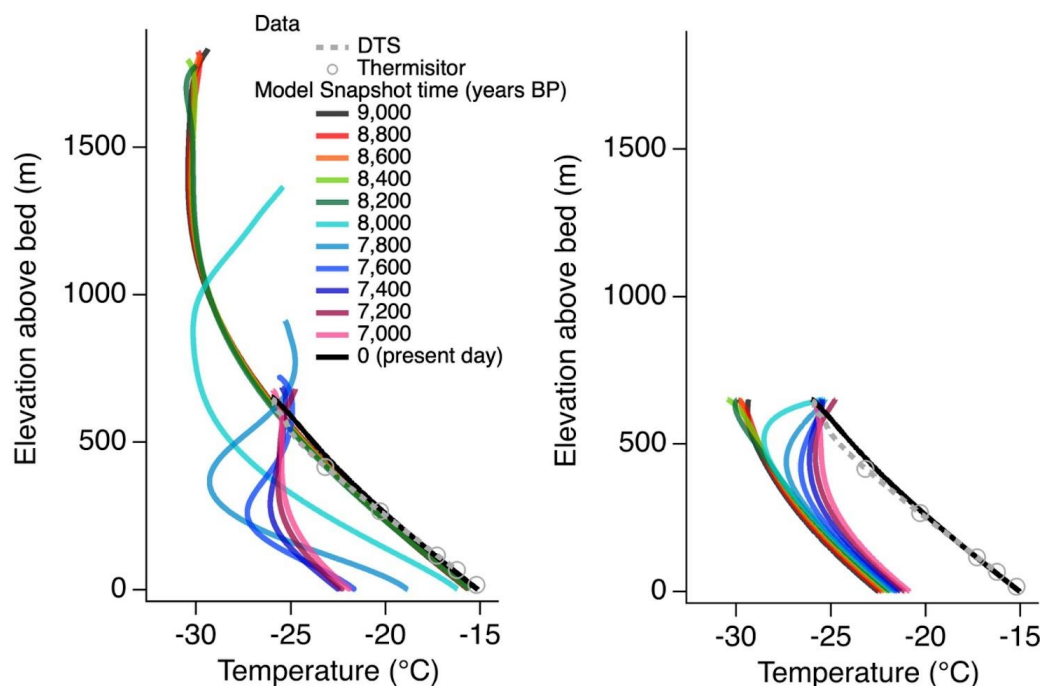
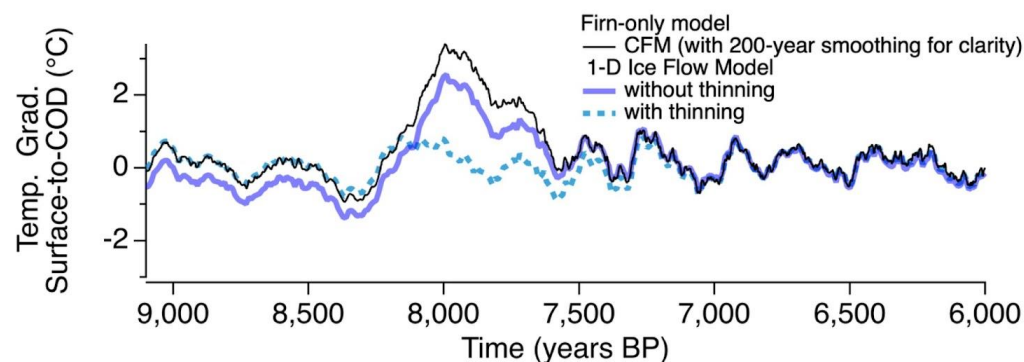
To force the model we use the same surface temperature, accumulation and ice thickness in our CFM experiments but include a  $\sim 100,000$  year spin-up under glacial conditions followed by transient simulation from 25,000 years BP to present day. The model is run with a timestep of one year and discretized with 1,000 boxes in the depth domain. The shape function employs a Lliboutry (1979) analytical function with parameter of  $p=3$ . The geothermal heatflux is held constant at 45 mW per  $m^2$ . Note this value is slightly lower than the preliminary inversion of geothermal heatflux presented in (Mulvaney et al., 2021) of  $\sim 47.5$

91 mW per m<sup>2</sup> based on early estimates of surface temperature, accumulation and thinning - all of which were assumed to be  
 92 constant in time. Our results suggest that thinning during the early Holocene could have a minor influence on the present-day  
 93 borehole temperature profile but an outstated influence if thinning occurred in the later Holocene (past few thousand years).  
 94  
 95  
 96

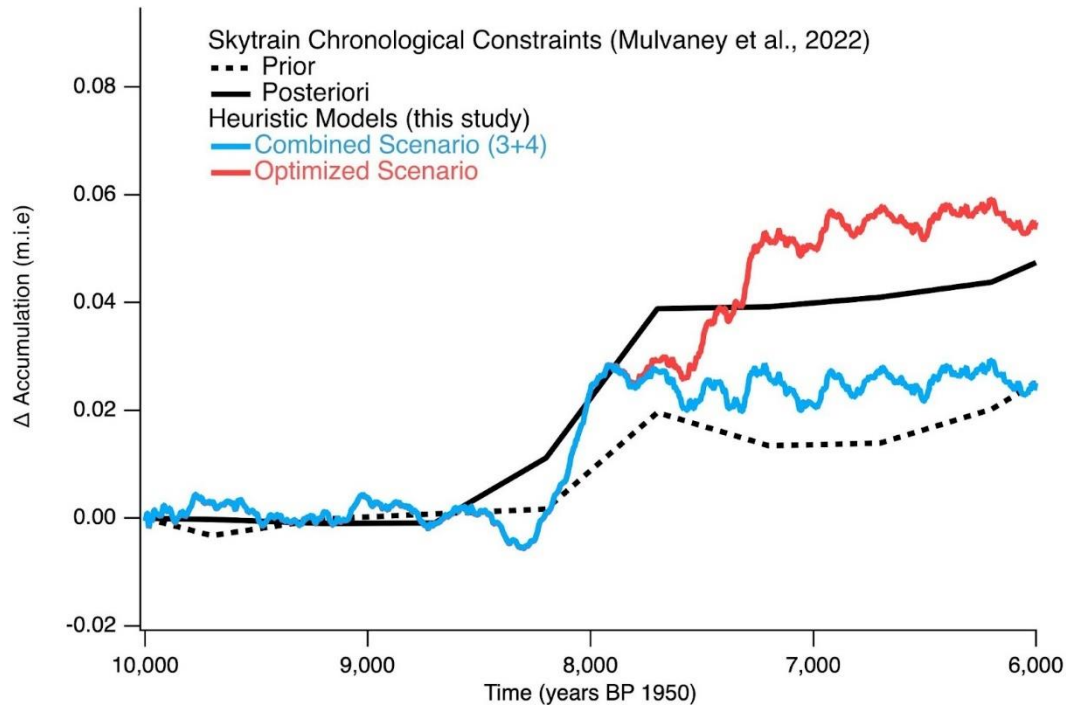
97

98 **Supplement Figure 3: Comparison of measured  $\delta^{15}\text{N}$  (top panel) and N excess (bottom panel) data from Skytrain ice**  
 99 **core alongside predicted scenarios of  $\delta^{15}\text{N}$  and N excess change using the Community Firn Model. Scenario 1**  
 100 **corresponds to a temperature change only scenario, Scenario 2 accumulation change only, Scenario 3 temperature and**  
 101 **accumulation change, and Scenario 4 with horizontal divergence only.**





**Supplementary Figure 4: Figure showing the evolution of temperature gradient using the 1D borehole temperature model. The upper panel shows the firn column temperature gradient evolving through the 8 ka time period, in scenarios both including and excluding our observed firn column thinning. Also shown is the same temperature evolution in the firn predicted in the CFM, which does not include thinning, to demonstrate agreement between the models under these conditions. Although thinning reduces the temperature gradient in the firn column, it does not reverse the temperature gradient as our measured N excess initially indicated. The lower panels show how the temperature gradient evolves through the full borehole in the 1D model scenarios with (left) and without (right) thinning, alongside the measured borehole temperature profile at Skytrain Ice Rise (Mulvaney et al., 2021).**



**Supplementary Figure 5: A comparison of changes in accumulation across the 8.0 ka event from this study in our combined scenario with a single ramp in accumulation (blue) and our optimized scenario with a second ramp that coincides a possible ice shelf breakup. For comparison we show previous work using the Paleochron model (Mulvaney et al., 2022) in which accumulation used a prior constraint (dash black line) and also derived a posteriori (solid black line) using chronological tie points and a constant thinning function.**

## References

- Cuffey, K. and Paterson, W. S. B.: The Physics of Glaciers, 4th Edn., Oxford, UK, Butterworth-Heinemann, <https://doi.org/10.3189/002214311796405906>, 2010.
- Jordan, T. A., Martin, C., Ferraccioli, F., Matsuoka, K., Corr, H., Forsberg, R., Olesen, A., and Siegert, M.: Anomalously high geothermal flux near the South Pole, Sci Rep, 8, <https://doi.org/10.1038/s41598-018-35182-0>, 2018.
- Lliboutry, L.: A critical review of analytical approximate solutions for steady state velocities and temperatures in cold ice sheets, Z. Gletscherkde. Glazialgeol., 15, 135–148, 1979.
- Mulvaney, R., Rix, J., Polfrey, S., Grieman, M., Martin, C., Nehrbass-Ahles, C., Rowell, I., Tuckwell, R., and Wolff, E.: Ice drilling on Skytrain Ice Rise and Sherman Island, Antarctica, Ann Glaciol, 62, 311–323, <https://doi.org/10.1017/aog.2021.7>, 2021.